Characterizing and Modeling Exciton Dissociation in Polythiophene

Presented by Andrew Mueller

In partial fulfillment of the requirements for graduation with the
Dean's Scholars Honors Degree in Biochemistry

_____ _____

Dr. Peter J. Rossky — Date
Supervising Professor

_____ _____

Dr. John F. Stanton — Date
Honors Advisor in Chemistry and Biochemistry

I grant the Dean's Scholars Program to (check all that apply):

____ Post a copy of my thesis on the Dean's Scholars website

____ Keep a copy of my thesis in the Dean's Scholars office for Dean's Scholars to read

Characterizing and Modeling Exciton Dissociation in Polythiophene

Department: Chemistry and Biochemistry

_____

Andrew Mueller

_____ _____

Signature Date

_____

Dr. Peter J. Rossky

_____ _____

Signature Date

Abstract

Exciton dissociation, the separation of an electron and hole upon excitation by radiation, is studied in the conjugated polymer polythiophene (PT). Based on data from semi-empirical simulations of exciton dissociation in PT, a dissociation distance parameter and the radius of gyration are calculated for the excited state electron and hole for different chain lengths of polymers. These characteristics are studied in relationship to themselves and each other to glean insight into the process and details of dissociation. It is learned that after the exciton is created, the length of the polymer that it spans is dependent on the chain length of the polymer. Also, it is discovered that the exciton changes in size in a consistent fashion, creating a pulsating effect with a consistent pulsating frequency.

In addition, a novel course-grained model for simulating exciton dissociation is created and implemented based solely on an effective interaction energy potential between the exciton cloud and the torsional angles between the rings of the polymer. The parameters for this model are chosen based off of the behavior seen in the semi-empirical calculations. After applying this new model to new configurations of the polythiophene polymer, the results are compared to results of the mixed quantum-classical simulations on the same configurations to show reasonably accurate prediction in the distribution of the exciton along the polymer.

Background

It is advantageous for optoelectronic devices, such as solar (photovoltaic) cells, to be made from organic materials rather than from metals, as plastics are more flexible, easier to produce, and cheaper to manufacture[1]. The best known candidates to use for the conducting material in these organic solar cells are long, conjugated polymers that can be printed onto very thin films and that can support proper energy transfer within their π-bond framework[2]. One such example of an organic, conjugated polymer is polythiophene (PT), shown below.

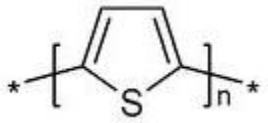

Figure 1. A polythiophene monomer.

Upon exposure to the correct frequency of UV light, the electronic state of PT is promoted to an excited state. The resulting change in electron configuration about the PT molecule results in the creation of a "hole," a positively-charged region void of the former negatively-charged electron density[3]. Together, the electron (e^-) and the hole (h^+) make up the exciton. Under appropriate conditions, the electron and hole can separate, and if a molecule of acceptor material is nearby, this separation can span across the two molecules. Recombination of the exciton within the donor molecule provides the energy transfer that can be utilized to perform the work necessary for some electrical or mechanical devices[4].

The characteristics of the individual donor and acceptor molecules can be studied experimentally, but this has been proven to be difficult due to a

tendency for the molecules to aggregate, even in very dilute solutions[5]. As a result, it has proven beneficial to study these molecules with computer simulations[6]. For this particular study, the computer simulation data was generated with mixed quantum/classical (MQC) simulations performed on the PT (donor) molecule according to the procedure outlined in Sterpone, et al[7]. This method uses a nonadiabatic molecular dynamics model with molecular mechanics employed for the polymer backbone, and a QCFF/PI framework with a semi-empirical Pariser-Parr-Pople (PPP) Hamiltonian to describe the π-electron system. During excitation, the transitions between the ground and excited electronic states are directed using the surface-hopping method[8].

Studying the behavior and characteristics of the exciton as it is created and as it separates can lead to increasing the overall efficiency of energy transfer in organic photovoltaic devices by identifying environments, geometries, conformations, or modifications that increase exciton dissociation[9]. The properties focused on in this study are an exciton dissociation parameter (d) and the radius of gyration (Rg) of the exciton, and are further defined later on in the Methods section of this paper.

Given that the MQC simulations described above are labor intensive and require significant computation time, even despite being semi-empirical, it is appealing to construct a simpler model that produces similar results in terms of exciton dissociation distribution along a conjugated polymer. There are many simple models currently in use, but the simplest and arguably most successful was developed by Yaliraki and Silbey[10]. Their model treats a polymer as a collection of monomers in one of two relative configurations to each other: planar or antiplanar. This results in distinct regions of planarity on the polymer chain, as shown in Figure 2 below.

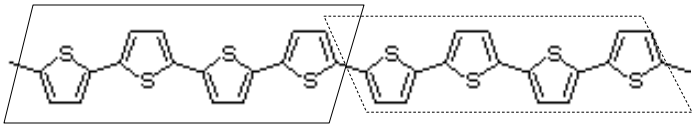

Figure 2. Planar regions in a PT polymer in the Yaliraki and Silbey model

However, there are two major shortcomings with this approach, the most notable being the requirement for selecting a specific cutoff angle that determines the planarity between two rings. Varying the selected angle can change the lengths of the conjugated sections of the polymer, and thus the outcome of a simulation using this model. As a result, the model is dependent not only on the conformation of the polymer, but the cutoff angle as well. Furthermore, this model minimally describes the interaction between the exciton and the polymer other than the fact that an exciton has a great tendency to localize its density within a planar region. Thus, a model which takes into account the orientation of each individual ring in the polymer relative to its neighbor(s) would be more accurate and more widely applicable across different conjugated systems. It is the goal of this study to provide such a model, one that relies on only a "kinkfield" to produce an accurate exciton density distribution quickly and without intensive calculations. The kinkfield that is input into the model is the distribution of torsional angles between monomeric rings on a given polymer, thus representing the extent to which the polymer is kinked in each location along its length. The basic formulation of this model is based on the creation of an effective interaction potential between the exciton cloud and torsion/dihedral angles between monomer rings. If successful, it would be a much improved coarse-grained model that could be mapped directly onto atomic systems and thus applied to any conjugated polymer system.

Methods

Exciton dissociation is defined here as the spatial separation of the electron and the hole on the polymer chain. Once they are created and separated, the positions of the electron and hole are defined as the center of charge of each cloud of density, weighted by their respective densities at each position point. Mathematically this is represented as

$$r_e(t) = \sum_i^N \rho_{e,i}(t) r_i(t), \quad (1)$$

where $r_i(t)$ is the position along the polymer of π-atom i at time t, and N is the number of rings (monomers) in the polymer. The center of charge for the hole is analogously defined. Finally, the exciton dissociation distance, $d(t)$, between the two is defined as

$$d(t) = |r_e(t) - r_h(t)|. \quad (2)$$

When examining the exciton dissociation in the conjugated PT polymer, a parameter was needed to determine the width of the electron and hole individually. The radius of gyration (Rg) is a measure of how spread out (delocalized) the electron or hole is about its weighted center (calculated above in (1)). It is defined as

$$Rg_e(t) = \sum_i^N \rho_{e,i}(t)\{r_i(t) - r_e(t)\}, \quad (3)$$

and can be applied in a similar manner to the hole as well. It does not need to be normalized as the quantity ρ is already normalized to a total density value of 1 in the MQC simulations.

For the novel exciton model, the derivation for the effective interaction potential is below. The relationship that is assumed and will be tested is that ρ and $cos(\phi)$ are coupled linearly with energy by a factor of γ. Thus, the equation for the potential energy $U(\{r\},\{\phi\})$ is

$$U(\{r\},\{\phi\}) = \int \gamma\ \rho(r)\ cos\big(\phi(r)\big)\ dr, \tag{4}$$

or, in summation form

$$U(\{r\},\{\phi\}) = \sum_n \gamma\ \rho(r_n)\ cos\big(\phi(r_n)\big). \tag{5}$$

Here, n is the kink number along the polymer chain and ρ is the amount of exciton that spans the torsional gap and is defined as the interpolation of the values of exciton density in the rings neighboring the gap, as follows

$$\rho(r_n) = \frac{\rho_n + \rho_{n+1}}{2}. \tag{6}$$

In the lower limit of a polymer chain having only one kink along its length, the probability of a value of exciton density spanning that kink given a torsional angle ϕ is

$$P(\rho|\ cos(\phi)) = \frac{1}{Z} Tr\big[\delta\big(\rho - \rho(r')\big) e^{-\beta U} \delta\big(cos(\phi) - cos\big(\phi(r')\big)\big)\big], \tag{7}$$

where Z is a normalization factor, Tr is the trace operator, and δ is a Dirac delta function. Incorporating the proposed potential energy relationship into the Boltzmann factor in (7) followed by rearrangement gives

$$P(\rho|\ cos(\phi)) = \frac{1}{Z} Tr\big[\delta\big(\rho - \rho(r')\big) e^{-\beta\gamma\rho(r')\,cos(\phi(r'))} \delta\big(cos(\phi) - cos\big(\phi(r')\big)\big)\big], \tag{8}$$

$$P(\rho|\, cos(\phi)) = \frac{e^{-\beta\gamma\rho\, cos(\phi)}}{Z} Tr\big[\delta\big(\rho - \rho(r')\big)\delta\big(cos(\phi) - cos\big(\phi(r')\big)\big)\big]. \qquad (9)$$

Here, the part of the equation acted on by the trace operator is merely the probability of exciton density with zero kinks on the polymer (shown in (10) as $P_0(\rho|\cos\phi)$), which does not depend on the angle ϕ, but only on ρ, as shown in (11).

$$P(\rho|\, cos(\phi)) = \frac{e^{-\beta\gamma\rho\, cos(\phi)}}{Z} P_0(\rho|\, cos(\phi)), \qquad (10)$$

$$P(\rho|\, cos(\phi)) = e^{-\beta\gamma\rho\, cos(\phi)} \frac{1}{Z} P_0(\rho). \qquad (11)$$

In order to get the desired linear relationship between ρ and ϕ for the derived model, we must take the ratio of one probability to another to get

$$\frac{P(\rho|\, cos(\phi_1))}{P(\rho|\, cos(\phi_2))} = e^{-\beta\gamma\rho(cos(\phi_1) - cos(\phi_2))}. \qquad (12)$$

Rearrangement gives

$$log \frac{P(\rho|\, cos(\phi_1))}{P(\rho|\, cos(\phi_2))} = \Gamma\rho(cos(\phi_1) - cos(\phi_2)). \qquad (13)$$

Thus, if this model describing this system is accurate, a plot of the log of the ratio of ρ given an angle ϕ versus a ρ value would give a linear relationship with a slope of $\Gamma(cos(\phi_1) - cos(\phi_2))$. The term Γ gives the effective energy in linear coupling in units of kT.

Ideally, different length polymer chains have the same Γ value, but this is unlikely since shorter chains have system size constraints that limit the exciton to a short section of monomers, regardless of the kinkfield of that polymer. Thus, the slopes (Γ values) need to be determined for each size of

chain length. A systematic approach to this is applied to generate consistent and relatable values and is detailed later in the Results section.

Once these slopes are found, the next step is to use them to solve for the effective energy $U(\{r\},\{\phi\})$ given different sets of kink angles found in the MQC simulations described in the Background above. The density distribution curve starts out set at a normalized Gaussian curve with a σ value of one ring, centered on the polymer chain. The energy of this initial distribution is calculated and is minimized given the proposed energy equation, the kink values, and the simulation gamma values, resulting in an exciton density distribution on the polymer. To compare it to the actual exciton distribution from the simulations, a parameter (dev) is created to represent the accuracy of the model in terms of how much the density values of the model deviate from the simulation values. The dev parameter is defined as

$$dev = \sqrt{\left(S(r_i(t)) - M(r_i(t))\right)^2}, \tag{14}$$

Where $S(r_i(t))$ and $M(r_i(t))$ are the simulation-produced density and model-produced density, respectively, at π-atom i at time t. The dev values of each atom in a polymer chain are averaged to get the dev for the whole polymer at time t.

Results and Discussion

The exciton dissociation parameter was calculated as discussed above for chain lengths of 6, 8, 10, 12, 14, and 16 monomers. A plot of the probability of values for d for the different polymer lengths is shown in Figure 3 Panel A. Panel B shows the same information but in a logarithmic scale.

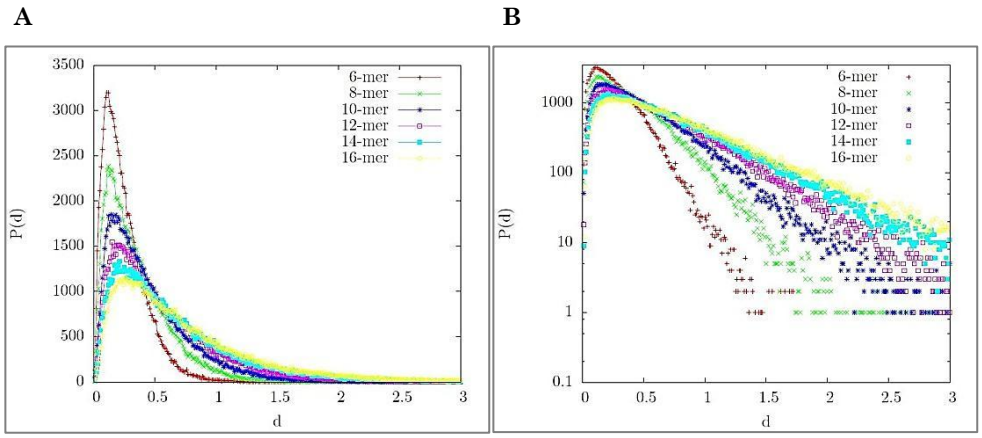

Figure 3. Probability of exciton dissociation distance, d, for different polymer lengths. Panel B is the same as Panel A but with a logarithmic scale.

According to this figure, the exciton is more likely to span a short distance, meaning the electron and hole stay relatively close together and associated with each other. This is likely due to a coulombic attraction between the negatively-charged electron cloud and the positively-charged hole cloud, as well as a spatial limitation of being forced to be localized in the same planar, conjugated segment as they were formed upon excitation. Comparing the curves for different length polymers, it is evident that the longer the polymer chain, the more likely the exciton is to be delocalized. There is more space on longer chains for delocalization, and the chances of having longer chains of conjugated rings is higher as the chain gets longer as well. Panel B allows for

the display of the trend continuing in the tails of the curves, as it becomes difficult to discern this on the linear plot in Panel A.

The radius of gyration, Rg, was calculated and plotted during each time step of the simulation. Figure 4 shows these results for the electron and hole at a chain length of 6 monomers (6mer), and for the electron only for chain lengths of 10 and 12 monomers. Logarithmic plots are included as well for enhanced view of the distribution of Rg values.

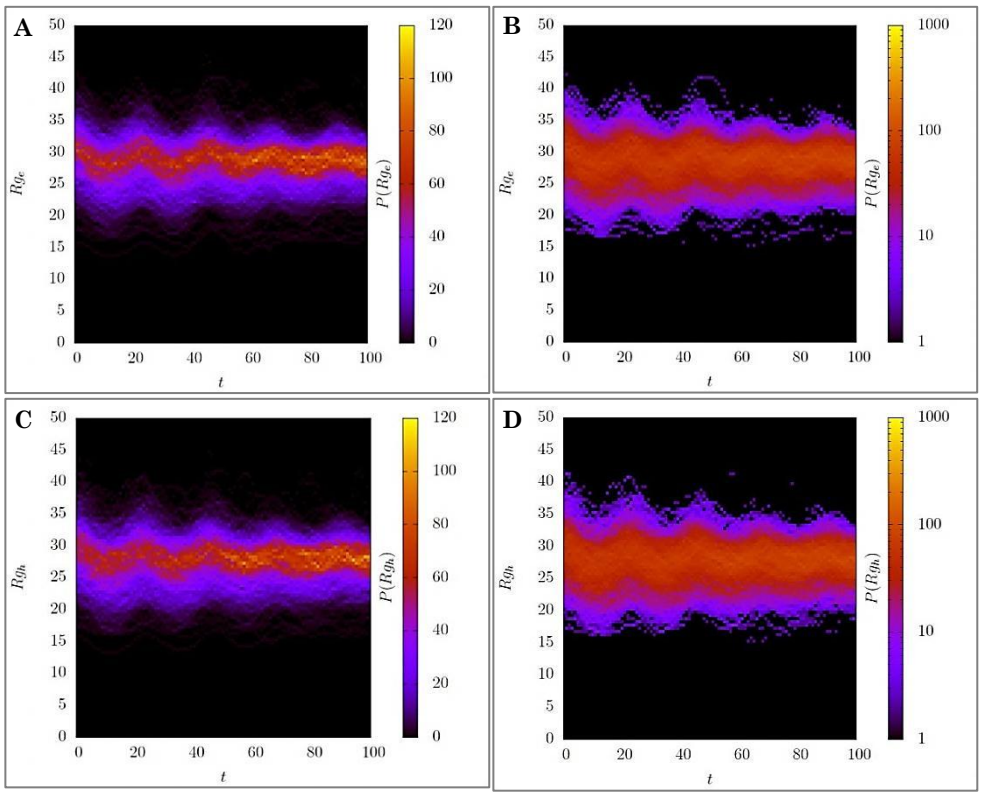

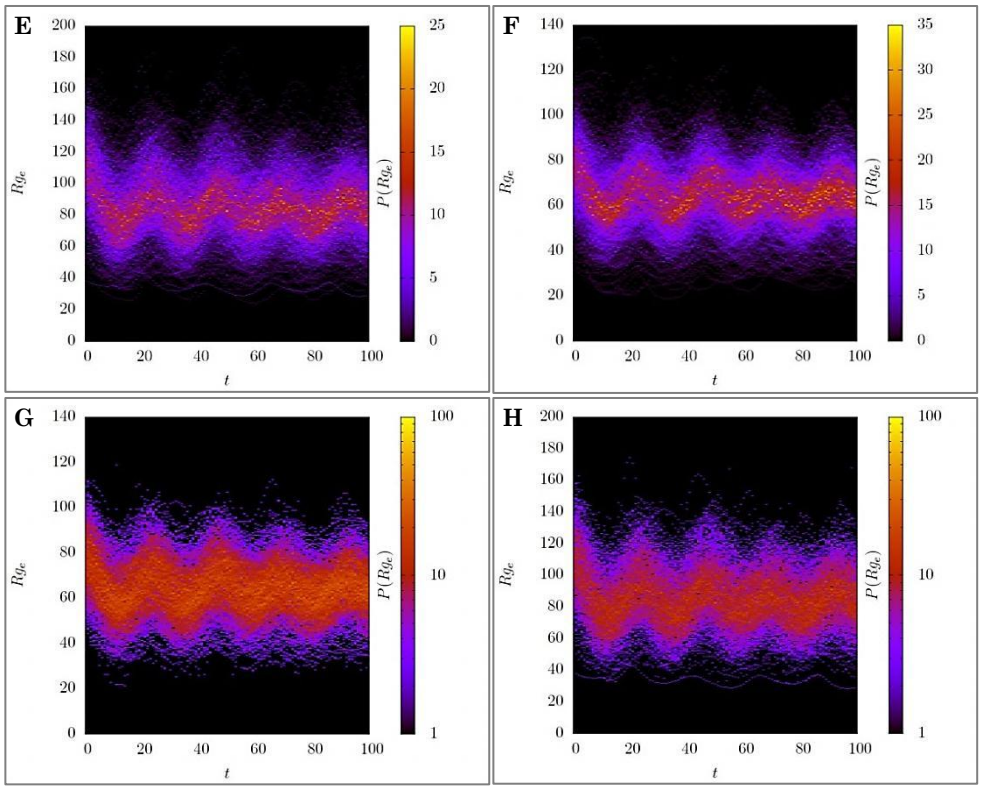

Figure 4. Probability of radius of gyration values in time. Panels on the right are in logarithmic color scales. Panels A and B show 6mer electron data. Panels C and D show 6mer hole data. Panels E and F show 10mer electron data. Panels G and H show 12mer electron data.

Comparing the pairs of Panel A and Panel B with Panel C and Panel D, it is noticed that the electron and hole behave similarly throughout the simulations. As a result, Panels E through H only display the Rg for the electron. Consistent with the conclusion drawn from Figure 3, Figure 4 shows a more diffuse exciton cloud as chain length increases, as the values for the radius of gyration, as well as the spread of the range of these values, increase with chain length. An interesting thing to note in all panels of Figure 4 is that the radius of gyration appears to be oscillating in time. Further inspection shows that the frequency of oscillation is consistent and independent of the

chain length and thus must be a property of the polymer chain and/or its environment. This was merely noted but not investigated further in this study.

Looking at the relationship between the electron and hole thus far, it appears as though they behave almost identically. To test this further, the radius of gyration for the electron and hole were plotted against each other at different chain lengths in Figure 5. The green diagonal line marks the graph locations of equal sized radii of gyration for the electron and hole.

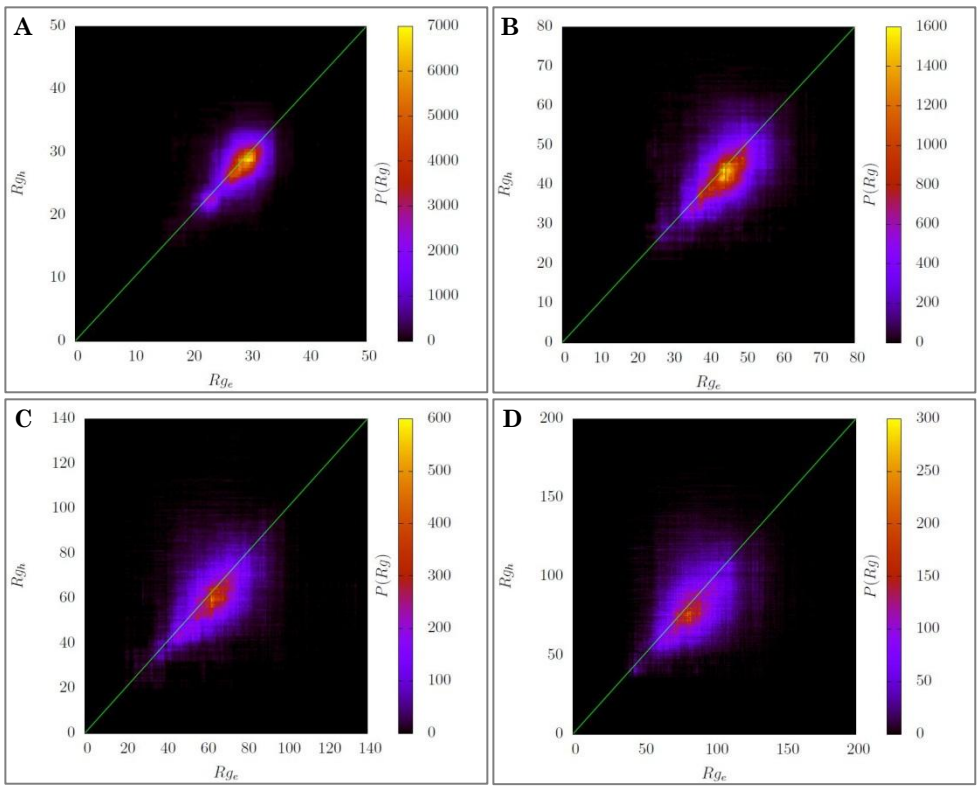

Figure 5. The radius of gyration of the electron vs. the hole for a PT 6mer (A), 8mer (B), 10mer (C), and 12mer (D).

On all four panels, the electron has a larger radius of gyration than the hole. This relationship becomes more exaggerated as the polymer chains get longer, as there are higher probabilities below the green line than above it. The

reason for this is unknown, and is currently being investigated by other members in the lab.

As for the simple coarse-grained model, the relationship between the torsion angle and the density distribution needed to be shown to be linear. A quick plot of (12) at one time step of one simulation for both a 6mer and a 12mer were made (Figure 6). From the two plots, it was determined that the relationship was close enough to linear to proceed on with further testing of the model.

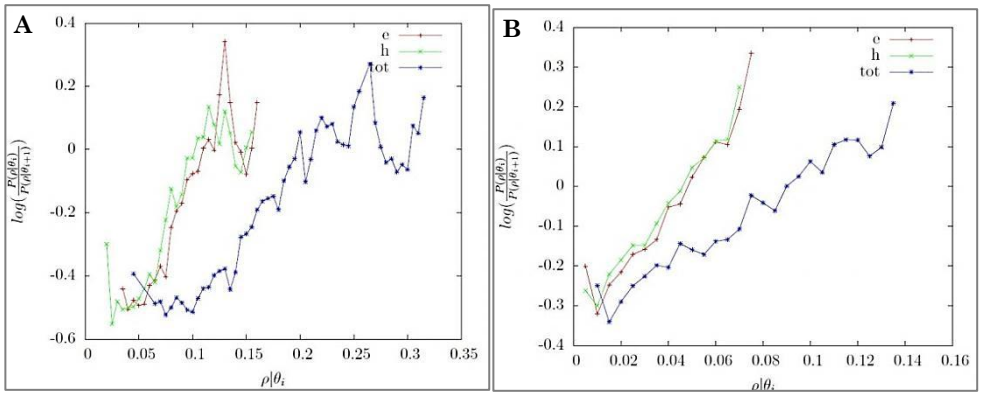

Figure 6. Snapshots of the linear relationships desired for our model, based on Equation (12), for a 6mer (A) and a 12mer (B). Trends are linear to a good extent.

The next step was to determine the value of energy coupling for this model, the term Γ in the derivation from the Methods section above. Using the same simulation data used for calculating d and Rg, plots were made of $P(\rho|\,cos(\phi))$ vs. $\rho\,|cos(\phi)$, which would give an indication of the validity of the model. These are shown in Figure 7.

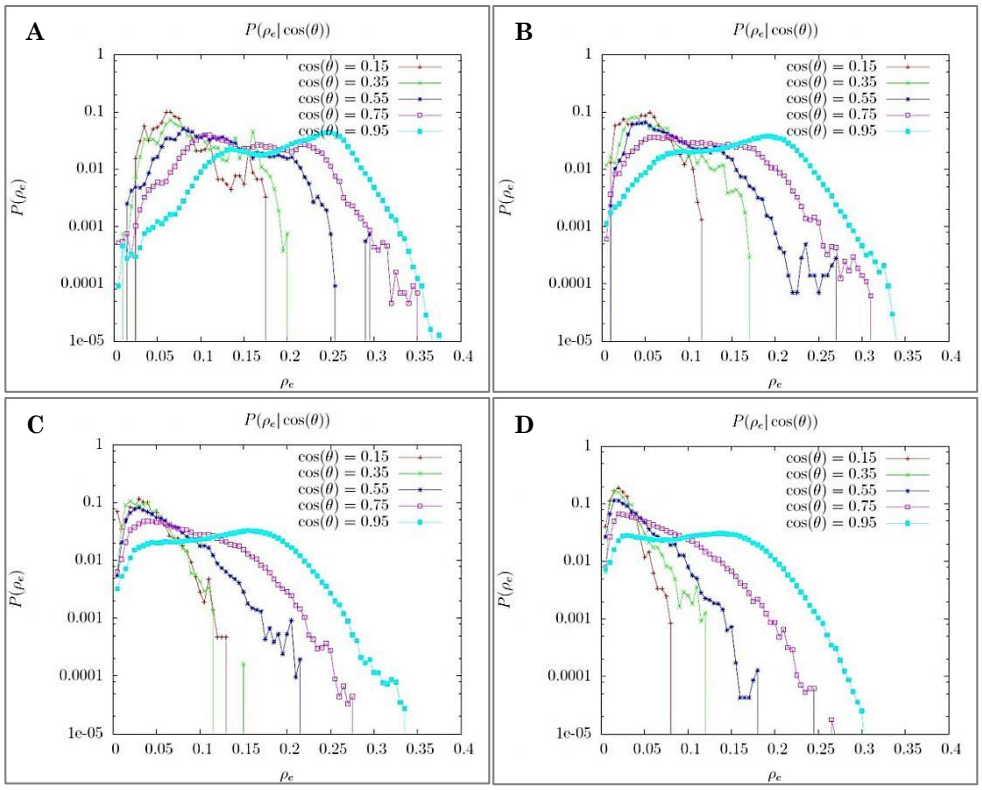

Figure 7. Probabilities of electron density spanning a torsion angle ϕ versus electron density for a 6mer (A), 8mer (B), 10mer (C), and 12mer (D). In the legend, θ is the same torsional angle as ϕ.

The curves in the plots show a consistent relationship to one another, once again hinting at the necessary linear relationship. From here, plots were made of (12) for all of the simulations and all of the chain lengths. These are displayed in Figure 8.

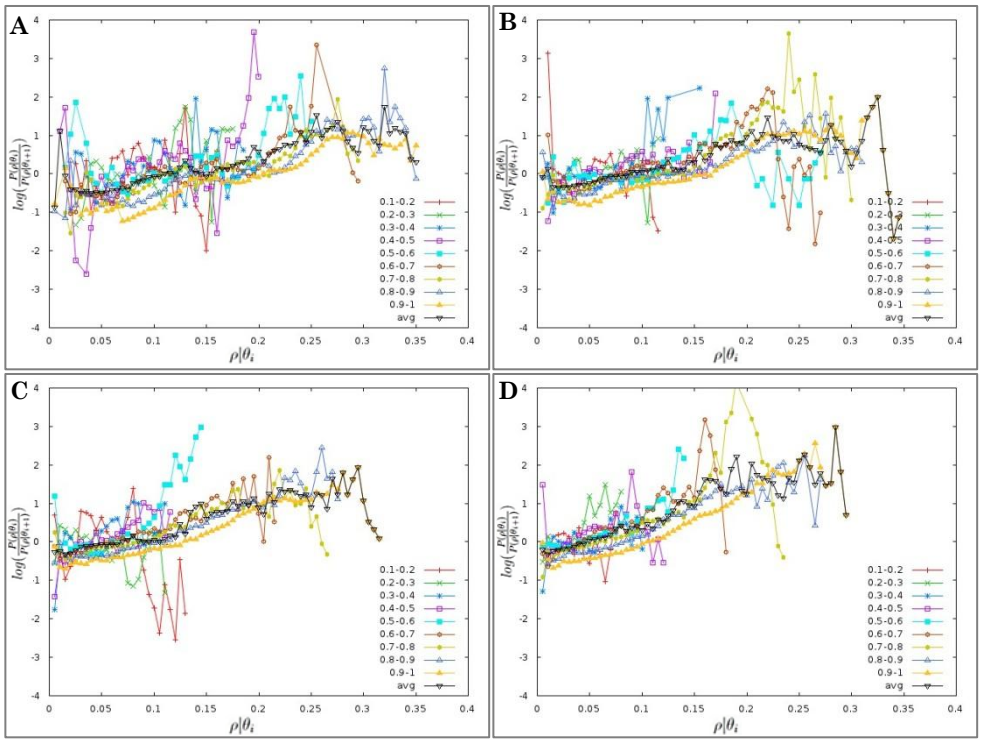

Figure 8. Plots of Equation (12) for 6mers (A), 8mers (B), 10mers (C), and 12mers (D). The legend numbers of the curves corresponds to the ratios of cosϕ values from 0.1 to 1 in increments of 0.1. The avg line is the average of all curves for that length polymer and is used to calculate Γ.

All of the panels in Figure 8 show a similar linear trend, particularly the lines that mark the average values of the curves. In order to obtain the most accurate Γ value, a systematic approach needed to be taken for each plot. The lines that represent the torsional angels closest to planar configurations are the most important, as they have more data points associated with them since the exciton prefers planar regions. Also, the curves are the most linear toward the lower end of the ρ axis, as there is less data as the density gets higher. This is due to the fact that the exciton prefers to delocalize across many kinks rather than be localized across one kink, thus lowering the density spanning each kink. As a result, linear regressions were performed on modified versions of

Figure 8 plots, which only included the three lines closest to planar configurations (0.7-0.8 to 0.9-1) and the range of ρ values between 0.02 and 0.22 because these ranges contained the most data. This has returned a value for Γ of 12.3. Although this value was determined under the consideration of only the most planar configurations, the model should still be applicable to configurations that are less planar without a noticeable loss of accuracy.

From this Γ value, the model was constructed as described in the Methods section. To test the accuracy of this model, it was applied to configurations found in simulation data, including longer length polymers than the ones used to determine the Γ value (14mers and 16mers). Figure 9 on the next page shows some comparative images that overlay the actual density profile of a polymer chain from the simulation with the density profile generated by the model. They are ordered by how accurate they are, determined by the dev parameter explained earlier.

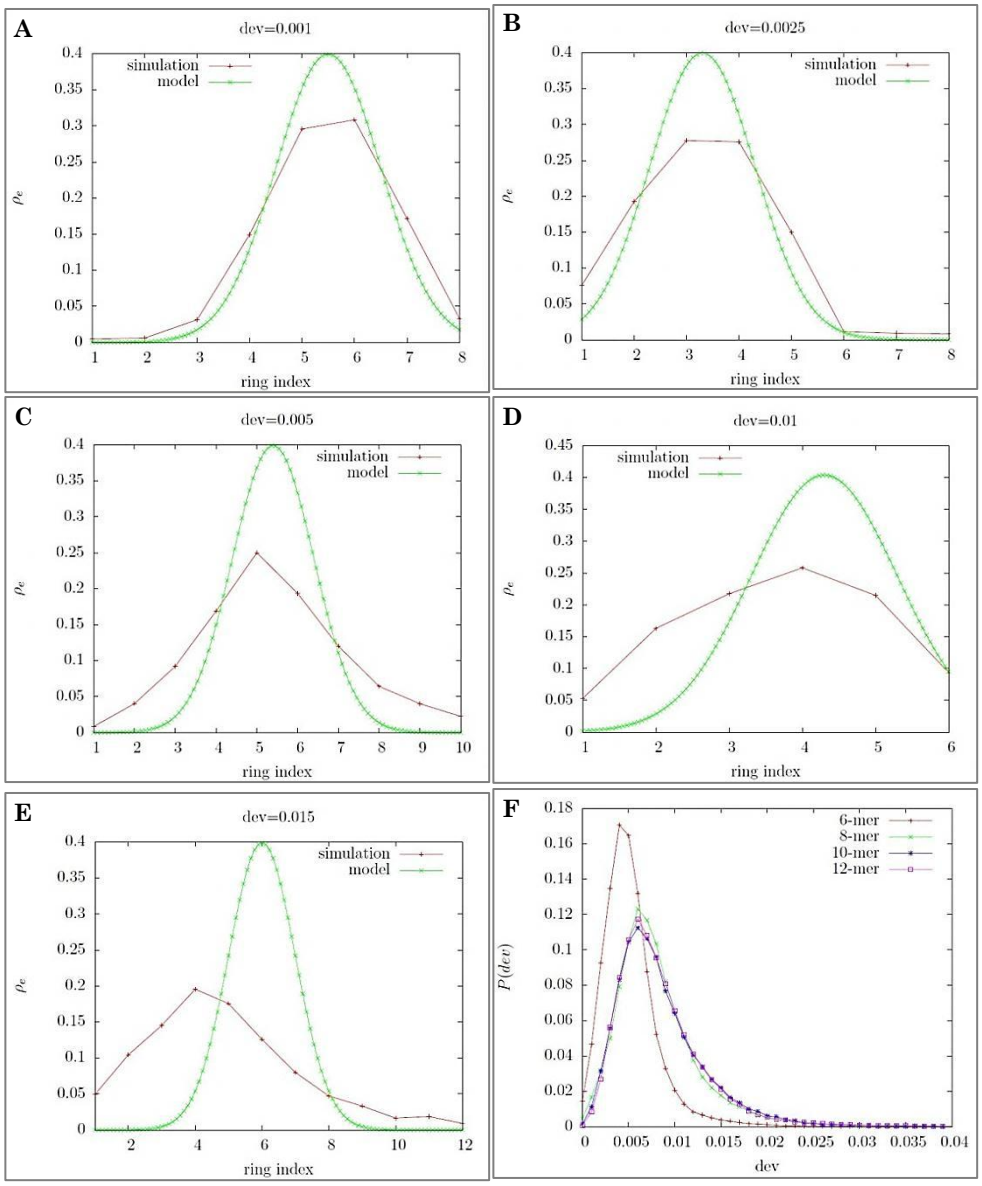

Figure 9. Graphical representations of electron and hole density distributions of both the MQC simulation and the model tested in this study. The dev values for Panels A through E represent the accuracy of the model compared to the simulation. Panel F shows the distribution of dev values for all timesteps of the simulations.

According to this figure, most of the models match up well with the simulations, with most of the simulations being about as accurate as the ones

pictured in Panels C and D. The position of the model curves is quite accurate in almost all cases. However, it is obvious that the width of the model curve is not as accurate and needs to be adjusted. This could be due to the fact that there is no penalty for the exciton to stay as narrow as possible. As it is in this study, the lowest energy conformation in this model would result from the exciton spanning the least number of kinks. However, in reality there are coulombic repulsions within the electron clouds and within the hole clouds, separately, causing them to delocalize to a greater extent and span more kinks.

The revised variation of this model currently being tested includes a coulombic term to make the model exciton distribution curve wider, as well as an additional gradient term to smooth out the steepness of the density curves. This gradient term is a result of the observation that the actual simulation data rarely approximates the shape of a Gaussian curve. However, it may eventually turn out that too many terms are needed to approximate exciton dissociation with a Gaussian shape as the basis curve. The goal of this study has been to only use the conformation of the polymer (its kinkfield) to generate results, and enumerating too many terms strays away from this goal. Thus, future changes may include alteration of the shape of the model curve from Gaussian to sinusoidal (a $\sin^2$ function). This would likely not need a coulombic or gradient term, which would suit our model's goals.

Acknowledgements

I would like to thank Dr. Peter J. Rossky for all of the kindness, patience, and mentorship that he has shown me throughout this entire research process. His support for me in all of my endeavors has been comforting and unwavering. I would also like to thank Dr. John R. Dowdle and Dr. Adam P. Willard for teaching me the ins and outs of computer programming and putting up with all of my questions. Additional gratitude goes out to the rest of the members of the Rossky Lab, who have made me feel at home and a part of the Rossky family.

References

(1) Yu, G.; Gao, J.; Hummelen, J. C.; Wudl, F.; Heeger, A.J. "Polymer Photovoltaic Cells: Enhanced Efficiencies via a Network of Internal Donor-Acceptor Heterojunctions", *Science*. **1995**, 270, 1789-1791.

(2) Bredas, J.-L.; Beljonne, D,; Coropceanu, V.; Cornil, J. "Charge-Transfer and Energy-Transfer Processes in π-Conjugated Oligomers and Polymers: A Molecular Picture", *Chem. Rev.* **2004**, 104, 4971-5004.

(3) Scholes, G. D.; Rumbles, G. "Excitons in Nanoscale Systems", *Nat. Mater.* **2006**, 5, 683-696.

(4) Bredas, J.-L.; Cornil, J.; Beljonne, D,; dos Santos, D. A.; Shuai, Z. "Excited-State Electronic Structure of Conjugated Oligomers and Polymers: A Quantum-Classical Approach to Optical Phenomena", *Acc. Chem. Res.* **1999**, 32, 267-276.

(5) Becker, K.; Da Como, E.; Feldmann, J.; Scheliga, F.; Csanyi, E. T.; Tretiak, S.; Lupton, J. M. "How Chromophore Shape Determines the Spectroscopy of Phenylene-Vinylenes: Origin of Spectral Broadening in the Absence of Aggregation", *J. Phys. Chem. B.* **2008**, 112, 4859-4864.

(6) Bedard-Hearn, M. J.; Sterpone, F.; Rossky, P.J. "Nonadiabatic Simulations of Exciton Dissociation in Poly-p-phenylenevinylene Oligomers", *J. Phys. Chem. A.* **2010**, 114, 7661-7670.

(7) Sterpone, F; Bedard-Hearn, M.J.; Rossky, P.J. "Nonadiabatic Mixed Quantum-Classical Dynamic Simulation of π-Stacked Oligophenylenevinylenes", *J. Phys. Chem. A.* **2009**, 113, 3427-3430.

(8) Tully, J.C. "Molecular Dynamics with Electronic Transitioins", *J. Chem. Phys.* **1990**, 93, 1061-1071.

(9) Schwarts, B.J. "Conjugated Polymers as Molecular Materials: How Chain Conformation and Film Morphology Influence Energy Transfer and Interchain Interactions", *Annu. Rev. Phys. Chem.* **2003**, 54, 141-172.

(10) Yaliraki, S. N.; Silbey, R. J. "Conformational Disorder of Conjugated Polymers: Implications for Optical Properties", *J. Chem. Phys.* **1996**, 104, 1245-1253.